Supplementary Materials for

Mouse models of acute and chronic hepacivirus infection

Eva Billerbeck, Raphael Wolfisberg, Ulrik Fahnøe, Jing W. Xiao, Corrine Quirk, Joseph M. Luna, John M. Cullen, Alex S. Hartlage, Luis Chiriboga, Kalpana Ghoshal, W. Ian Lipkin, Jens Bukh, Troels K. H. Scheel, Amit Kapoor, Charles M. Rice*

correspondence to: ricec@rockefeller.edu

This PDF file includes:

Other Supplementary Materials for this manuscript includes the following:

Materials and Methods

Mice

C57BL/6J, BALB/c, NOD.Cg-*Rag1 IL2rg*^{tm1Wjl}/*Sz* (NRG) and B6;129-Mavs^{tm1Zjc}/J (Mavs$^{-/-}$) mice were obtained from the Jackson Laboratory. IFNAR knockout (A129) and IFNAGR knockout (AG129) mice were obtained from B&K Universal and miR-122 knockout mice were previously described (*8*). C57BL/6J, BALB/c, NRG, A129, AG129 and miR-122 KO mice were bred and maintained at the Comparative Bioscience Center of the Rockefeller University. All experiments in mice were in accordance with the NIH Guide for the Care and Use of Laboratory Animals and approved by the Rockefeller University Institutional Animal Care and Use Committees. Experiments with Mavs$^{-/-}$ mice were performed at North Carolina State University using protocols approved by the Institutional Animal Care and Use Committee.

Norway rat hepacivirus (NrHV) inoculum

Two novel rodent hepacivirus (RHV) species were identified during a metagenomic survey of zoonotic pathogens in New York City rats (*5*). We used samples of two wild rats (Rattus norvegicus) infected with different RHV species, termed RHV-rn-1 and RHV-rn-2, for initial phylogenetic analysis. We determined that the 5'UTR of RHV-rn-1 contains two miR-122 seed sites, while the 5'UTR of RHV-rn-2 had only one miR-122 seed site. Next, we infected four pairs of Sprague Dawley rats with RHV-rn-1 containing serum and liver homogenate i.v. All animals developed high-titer viremia, starting the first week post infection, and remained viremic for the study period of 6 months. All experiments in rats were performed at The Research Institute at Nationwide Children's Hospital using protocols approved by the Institutional Animal Care and Use Committee.

A serum sample of one chronically infected adult female was then used for infecting laboratory mice. Throughout this study we refer to RHV-rn-1 as NrHV.

To produce virus stocks for this study, 4-week-old NRG mice were infected with 10^4 genome equivalents (GE) rat-serum-derived NrHV or NrHV that was previously passaged through NRG mice (serial passage pool, see fig. S1). NrHV titers of virus stocks were determined by RT-qPCR as described below. Stocks were stored at -80°C.

NrHV infection of mice

4-8 week old female and male mice were used for experiments. To determine age-dependent virus clearance 4-, 8-, 12-week and 6 months old mice were used. Mice were either infected with the original rat NrHV inoculum or with NrHV derived from NRG serum (serial passage pool, see fig. S1). Mice were infected intravenously with 10^4,10^3,10^2 or 10^1 NrHV GE by retro-orbital injection. For secondary challenge experiments mice were infected using the same route of infection and the same inoculum as for the primary infection.

RNA isolation and NrHV RT-qPCR

Viral RNA from mouse serum was isolated using the High Pure Viral Nucleic Acid Kit (Roche). For RNA isolation from mouse tissue, fresh tissue was homogenized using metal bead homogenization in a TissueLyser LT (Qiagen). Total RNA from homogenized tissue was isolated using the PureLink RNA Mini Kit (Ambion). Mouse serum and RNA

were stored at -80°C. NrHV RNA was detected and quantified by one-step RT-qPCR using TaqMan Fast Virus 1-Step Master mix (Applied Bioscience) using a LightCycler 480 (Roche) with the following protocol: 50°C for 30 min, 95°C for 5 min followed by 40 cycles of 95°C for 15 sec, 56°C for 30 sec and 60°C for 45 sec. The sequences of NrHV E1 specific primers used for this protocol were:

Sense: GGCTGTGTCATCTGCGAGCA,

Anti-sense: CGACGAAGTCTATATGGTGGGC

Probe: [6-FAM]GGCCCCATGGTATCCAGGTCACCGCACTA[BHQ1a-6FAM]

An NrHV standard curve was generated from in vitro transcribed RNA from a plasmid encoding the partial NrHV E1 sequence. After in vitro transcription, the RNA was quantified and diluted to concentrations ranging from 10^8-10^1 GE/µl.

Viral sequence analysis

Full-Length ORF Amplification of NrHV genomic RNA: Total RNA was extracted from 20 µl serum using TRIzol® LS Reagent (Thermo Fisher Scientific). Reverse transcription (RT) was performed with Maxima H Minus Reverse Transcriptase (Thermo Fisher Scientific). Samples were pre-incubated in the absence of the RT enzyme at 65 ºC for 5 min prior to the reaction. RT was carried out at 50 ºC for 2 h in the presence of RNase inhibitors (Promega) using 0.1 µM primer TS-O-00319. Amplification of the complete ORF was performed using Q5® High-Fidelity Hot start DNA Polymerase (NEB), including high GC Enhancer, and the primer pair TS-O-00318 and TS-O-00361 (0.5 µM each). Prior to sequencing (Macrogen), amplified DNA was purified using DNA Clean & Concentrator (Zymo Research). Primer sequences:

TS-O-00319: GCTTCCTGGAGCGGGCTAGATACTG, Position 9116R

TS-O-00361: AGGTGAAGGGGGCATCGATG, Position -308F

TS-O-00318: CCAAGCCCCAATGCCGTCCGGCACCGCTGCCCTTTTCGG, Position 9028R (Nucleotide numbering according to ORF).

Full-ORF cloning for linkage analysis: Prior to TOPO XL cloning (Thermo Fisher), amplified full-ORF DNA was gel purified using Zymoclean Gel DNA Recovery Kit (Zymo research) and A-overhangs were generated using the native Taq polymerase (Thermo Fisher) for 30 min at 72 ºC. Clones were sequenced following restriction analysis to screen for correct inserts (Macrogen).

Deep Sequencing analysis: Libraries were prepared by NEBNext DNA Ultra II kit using dual indices and sequencing on a Illumina Miseq using 150 PE V2 kit (Illumina). BWA-MEM was used for mapping. Samtools, VarScan 2 and VCFtools were applied in succession in order to generate consensus sequences from the mapped reads. Finally, a combination of Samtools Lo-Freq and SnpEff was used for downstream SNP analysis as previously described (*21*). For codon analysis, the VirVarseq pipeline was applied (*22*).

Phylogenetic analysis: NrHV ORF sequences were aligned by the MAFFT algorithm using Geneious R7. jModelTest 2.1.5 was used to analyse the alignment, which found the general time reversible model (GTR) with inverse gamma to be the most suitable substitution model. Phylogeny was inferred using MrBayes v3.2.1, on a full-length ORF sequence alignment (GTR, nst=6 rates=invgamma). The Markov chain Monte Carlo algorithm was run for 10,000,000 iterations, with a sampling frequency of 7200, using two independent runs with three chains each in order to check for

convergence. Burn-in was set at 25% of samples. The consensus tree was visualized in FigTree v.1.4.3 (*21*).

Leukocyte isolation

Mice were sacrificed at one time point prior to infection and at multiple time points post infection and leukocytes were immediately isolated from blood, liver and spleen. Blood-derived leukocytes were isolated from heparinized blood by Ficoll-density gradient (Cellgro) centrifugation (20min, 2000rpm, 20°C). The liver was perfused with cold PBS (Gibco) prior to leukocyte isolation. The perfused liver tissue was minced and digested with collagenase IV (HBSS, 0.01% collagenase IV, 40mM HEPES, 2mM $CaCl_2$ and 2U/ml DNAse I) for 20min at 37°C followed by homogenization through a 100µm cell strainer (BD Biosciences). Leukocytes were subsequently isolated from liver cell suspension by Ficoll-density gradient centrifugation (20min, 2000rpm, 20°C). The spleen was minced and digested with collagenase IV (HBSS, 0.01% collagenase IV, 40mM HEPES, 2mM $CaCl_2$ and 2U/ml DNAse I) for 10min at 37°C. A leukocyte suspension was prepared from the digested spleen by homogenization through a 100µm cell strainer. Isolated leukocytes from blood, liver and spleen were washed twice in PBS and directly analyzed.

Flow cytometry

For surface marker staining, cells were plated on a 96-well-plate, blocked for 10 min at 20°C with anti-mouse Fc-block (BD Biosciences), stained with appropriate antibodies for 15 min at 20°C, washed twice with staining buffer (PBS with 1% FCS) and fixed with 4% paraformaldehyde. For staining of intracellular proteins, cells were first stained for surface markers followed by permeabilization (15min, 4°C, Transcription Factor Staining Buffer Set, eBioscience) and staining for intracellular proteins (30 min, 4°C). For staining of intracellular cytokines cells were stimulated with 5ng/ml PMA and 500ng/ml Ionomycin (Sigma) in the presence of brefeldin A (eBioscience). After 5h of incubation at 37°C cells were stained for surface markers, permeabilized (Transcription Factor Staining Buffer Set, eBioscience) for 15 min at 4°C and stained for intracellular cytokines (30 min, 4°C). For the analysis of total cell numbers CountBright absolute counting beads (Molecular Probes) were used according to the manufactures instruction. FACS analysis was performed using a LSRII flow cytometer (BD Biosciences). Flow Jo Software (Treestar Inc.) was used for data analysis.

Analysis of antigen-specific T cells

18mer peptides over-lapping by 11 amino acids covering the entire NrHV NS3 and NS4 proteins were generated (Genemed Synthesis Inc.) and pooled in 3 pools (2 NS3 pools, 1 NS4 pool) with a final concentration of 100µg/ml.

Leucocytes were isolated from blood, liver and spleen of C57BL/6J at day 9, 15, 21 and 200 post infection or at day 5 post reinfection. Cells were then plated on a 96-well-plate in medium (RPMI, 10% FCS, 1mM HEPES) and incubated for 18h at 37°C. Subsequently cells were stimulated with 1µg/ml of NrHV NS3-1, NS3-2, NS4 peptide pools or left unstimulated (control) for 5h at 37°C in the presence of brefeldin A. Cells were then stained for surface markers and intracellular cytokines as described above.

Antibodies

The following anti-mouse antibodies were used for flow cytometry: purchased from Biolegend: CD3 APC/Cy7 and Pe/Cy7 (145-2C11), CD44 Pacific Blue (IM7), CD62L FITC (MEL-14), CD8 Brilliant Violet 650 and PerCP (53-6.7), Tim-3 APC (RMT3-23), CD69 PeDazzle594 (H1.2F3), CD4 Alexa Fluor 700 and PerCP (GK1.5), CD4 Alexa Fluor 700 (RM4-5), NKp46 PerCP/Cy5.5 (29A1.4), CD80 FITC (16-10AI), B220 Brilliant Violet 510 (RA3-6B2), CD14 APC/Cy7 (Sa14-2), CD25 Brilliant Violet 510 (PC61), CD86 Pacific Blue (GL-1), F4/80 PE (BM8), Ly6C PerCP-Cy5.5 (HK1.4), Ly6G PeCy7 (IA8), CD138 APC (281-2), CD19 APC/Cy7 (6D5), CD11c PeDazzle594 (N418), ki67 PE (16A8), TNF-a PeDazzle594 (MP6-XT22), IFN-g APC (XMG1.2), GranzymeB Pacific Blue (GB11), CD49a APC (HMa1), CXCR6 Brilliant Violet 421 (SA051D1),Trail PE (N2B2). Purchased from eBioscience: CD127 Pe/Cy7 (A7R34), 2B4 PE (eBio244F4), CD49b PeCy7 (DX5), PD-1 PerCP/eFluor710 (RMP1-30), NK1.1 PE and Brilliant Violet 650 (PK136), CXCR5 Pe/Cy7 (SPRCL5), Eomes PeFluor610 (Dan11mag), FoxP3 Alexa Fluor 488 (FJK-16s), GATA-3 APC (TWAJ), T-bet PE (eBio4Bio), Perforin PE (eBioOMAN-D). Appropriate isotype controls were also purchased from Biolegend or eBioscience.

In vivo immune cell subset depletions

CD4+ T cells were depleted in C57BL/6J and BALB/c mice by intraperitoneal injection (i.p.) of 500µg/mouse per time point of an anti-CD4 depletion antibody (clone GK1.5, Bioxcell) and CD8+ T cells were depleted by i.p. injection of 500µg/mouse per time point of an anti-CD8 depletion antibody (clone 2.43, Bioxcell). Control animals were treated with 500µg/mouse per time point of rat IgG2b isotype control (clone LTF-2, Bioxcell). Time points of T cell depletion for all experiments are illustrated in fig. S6. CD4+ and CD8+ T cell depletion efficacy and kinetics of cell recovery were analyzed by flow cytometry. NK cells were depleted in C57BL/6J mice by i.p. injection of 250µg/mouse of anti NK1.1 antibody (clone PK136, Bioxcell) at day 2 prior to infection. NK cell depletion efficacy was determined by FACS analysis at day 9 and 15 post infection and was >98% in blood, spleen and liver. Control mice were injected with 250µg/mouse mouse IgG2a isotype control (clone C1.18.4, Bioxcell).

In vivo PD1-L blockade

PD-1L-blockade experiments were performed in C57BL/6J mice that were chronically NrHV infected after initial CD4+ T cell depletion. PD-1L was blocked by intraperitoneal injection of 250µg/mouse per time point of anti-PD-1L (clone 10F.9G2, Bioxcell). Control animals were treated with 250µg/mouse per time point of rat IgG2b isotype control (clone LTF-2, Bioxcell). Time points of PD-1L blockade for all experiments are illustrated in fig. S6.

Serum neutralization assay

10^4, 10^3 or 10^2 GE NrHV were incubated for 1h at 37°C with 5µl of serum from C57BL/6J mice that had previously cleared NrHV infection (post-clearance serum) or 5µl of serum from naïve mice (naïve serum). Post-clearance serum was derived from mice that were infected with the same NrHV inoculum (NRG adapted virus) that was subsequently used for the serum neutralization assay. Serum was collected from these

mice at week 10 p.i. and was confirmed positive for NS3 antibodies by LIPS assay (see below). Groups of naïve C57BL/6J mice were then infected with 10^4, 10^3, or 10^2 GE of post-clearance serum or naïve serum incubated NrHV. Viremia was analyzed at day 1, 3 and 5-post infection.

ALT assay

Alanine aminotransferase (ALT) levels in serum of mice were determined using an ALT activity assay Kit (Biovison) according to the manufactures instructions.

LIPS (luciferase immunoprecipitation system) assay

We utilized the LIPS technology for evaluating antibody response against NrHV in infected mice. A 240 amino acid fragment (positions 1139 to 1379) of the NrHV helicase protein (NS3) was subcloned downstream of Renilla luciferase (Rluc) using the pREN2 vector to express Rluc-fused viral antigen. A 96-well microtiter plate format of LIPS was employed to evaluate antibodies in the serum samples against virus helicase protein. For generating the master plate, serum samples of mice were diluted 1:10 in assay buffer A (20 mM Tris, pH 7.5, 150 mM NaCl, 5 mM $MgCl_2$, 1% Triton X-100) and then stored at 4°C until use. Additional buffer blanks were also included to monitor background binding activity of the assays. LIPS testing was initiated by adding 40 µl of buffer A, 10 µl aliquots of serum dilution (equivalent to 1 µl of serum) from the master plate, and 50 µl of the *Rluc*-antigen. Cos1 cell extract typically containing an equivalent of 10^7 light units (LU) were added to a polypropylene plate. After one hour incubation at room temperature with shaking, the mixture containing IgG antibody-antigen complexes was transferred to a microtiter filter plate containing protein A/G beads for one hour additional incubation. Next the filter plate was washed with buffer on a vacuum manifold to remove unbound *Rluc*–tagged antigens. LU were then measured using a luminometer following the addition of coelenterazine substrate. All LU data were obtained from the average of two wells and were not corrected for background protein A/G bead binding.

Histology

Tissues were prepared using standard histopathology techniques. Briefly, tissues were formalin fixed (3-4 days) transferred to 70% ethanol and processed using Leica Peloris with routine dehydration, clearing and infiltration schedule (50 minute steps). Tissues were paraffin embedded and sectioned at 4 microns. H&E staining was performed on a Leica ST5020 automated stainer and scanned with the Leica SCN 400F.

Statistics

Statistics were calculated using GraphPad Prism. Paired and unpaired students t-test were used to determine statistically significant differences.

Fig. S1

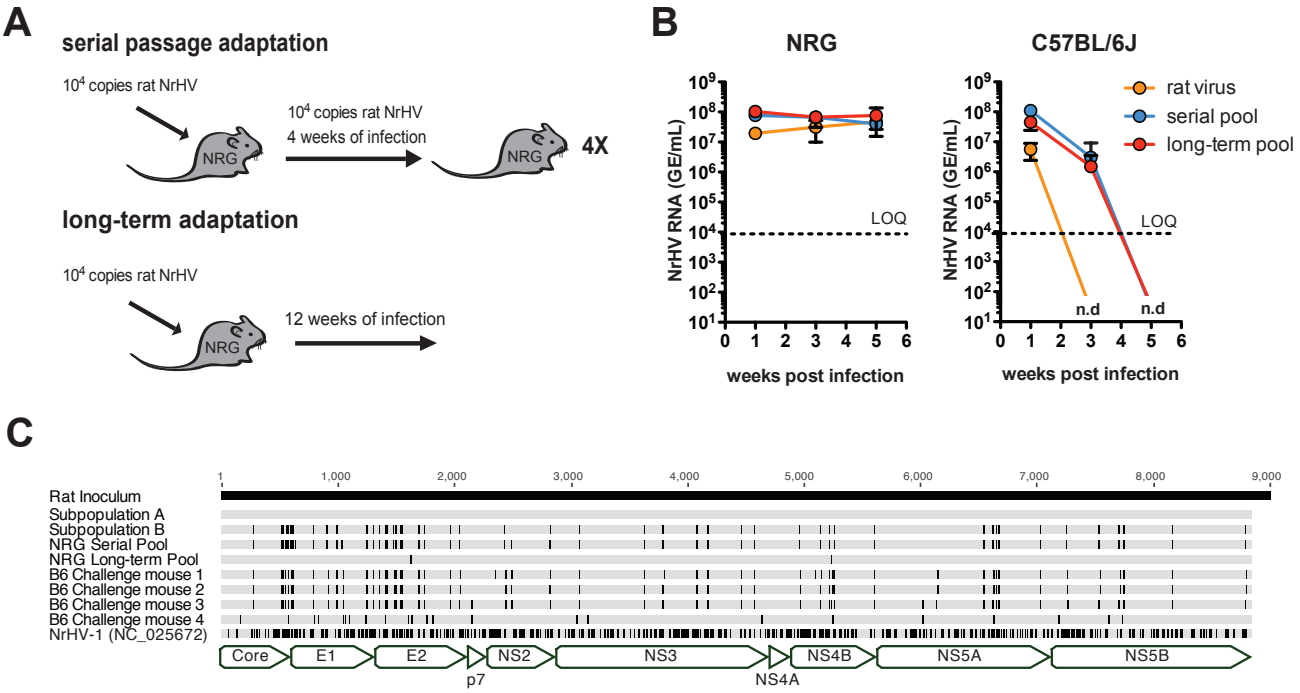

Changes in sub-population "B"

P179S*	R208E	T500A	I1661V
L180Y	T212A	R505W	N2214K
G183S	T422M	N518S	E2223V
P184T	E441G	G570R	Q2575R
F196V	S458P	V572A	K2586N
L199I	T477A	L586S	I2935T
T207S	K481E	A1397V	

* Present in rat, not in mice

Fig. S1. NrHV mouse adaptation, sequence comparison and selection of sequence variants during adaptation.

(A) Schematic of NrHV adaptation in NRG mice. Long-term adaptation: NRG mice (n=6) were infected with 10^4 GE rat-serum-derived NrHV for 12 weeks. Serial passage adaptation: NRG mice (n=9) were infected with 10^4 GE rat-serum-derived NrHV and sacrificed at week 4 p.i..The 9 independent lineages were consecutively passaged to naïve NRG mice for a total of 5 animals per lineage. (B) Naïve NRG and C57BL/6J mice were challenged with a total of $9x10^4$ GE of either the original rat NrHV inoculum, an equimolar pool of the 6 long-term passages or a pool of the 9 serial passages. (10 mice per group, mean ±SEM). (C) Schematic NrHV consensus ORF sequence alignment of the rat inoculum, the two identified sub-populations, NRG long-term and serial passage serum pools and four individual C57BL/6J mice challenged with the serial passage pool. The published NrHV-1 sequence from a wild-caught rat (5) is shown for comparison. (D) Phylogenetic relationship between full-ORF clones as well as consensus sequences of the inoculum and pools. In addition, the consensus sequences from individual animals (corresponding to Fig. 1C) are shown. (E) Selection of sequence variants in the NRG long-term and serial passage serum pools. The $\log_2$-transformed relative frequency between the NRG serum pools and the rat inoculum are shown for all amino acid variants. A pseudo-count of 0.5% was added to the deep sequencing data before calculation to reduce noise from low abundant variants. Dot size correlates to variant abundance in the two pools. Positions with consensus change (>50% abundance) in the serial passage pool are shown in red. To the right, consensus changes identified in sub-population “B” compared to “A” are shown. The complement data sets are shown in Supplementary Tables 1-2.

Fig. S2

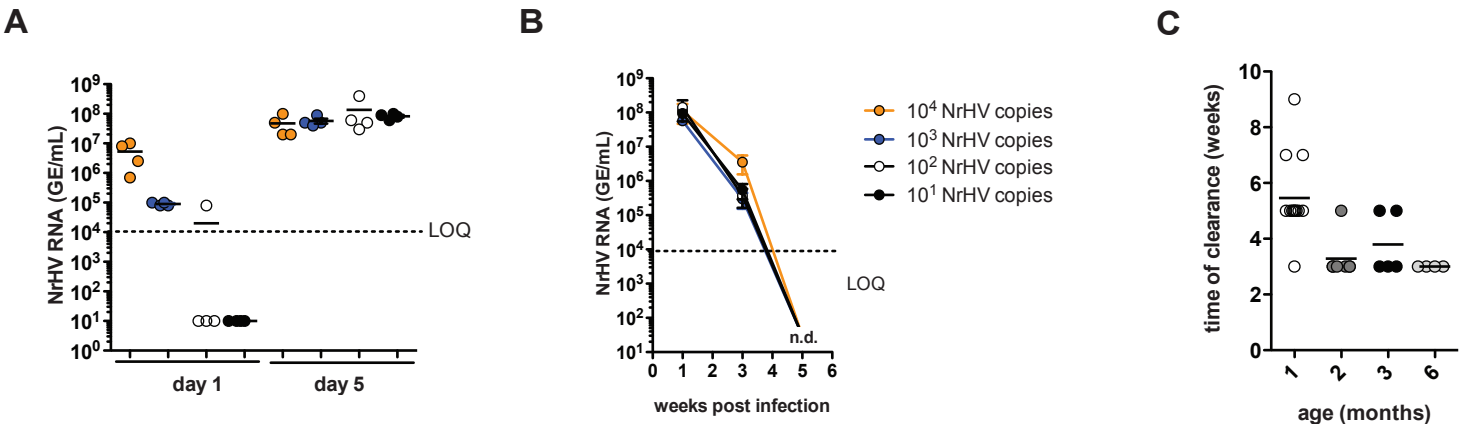

Fig. S2. NrHV infection with different inoculum doses and different age of mice.
(A-B) 4-week old C57BL/6J mice were infected i.v. with either 10^4,10^3,10^2 or 10 GE of NrHV. Viremia at day 1 and 5 p.i. is shown in (A) and the course of infection in (B). Representative data from 2 independent experiments with 4 mice per group (mean ±SEM) are shown. (C) C57BL/6J and BALB/c mice of different age (1-6 months) were infected i.v. with 10^4 GE of NrHV and time of viral clearance was determined. The graph shows combined results from both mouse strains, which behaved similarly.

Fig. S3

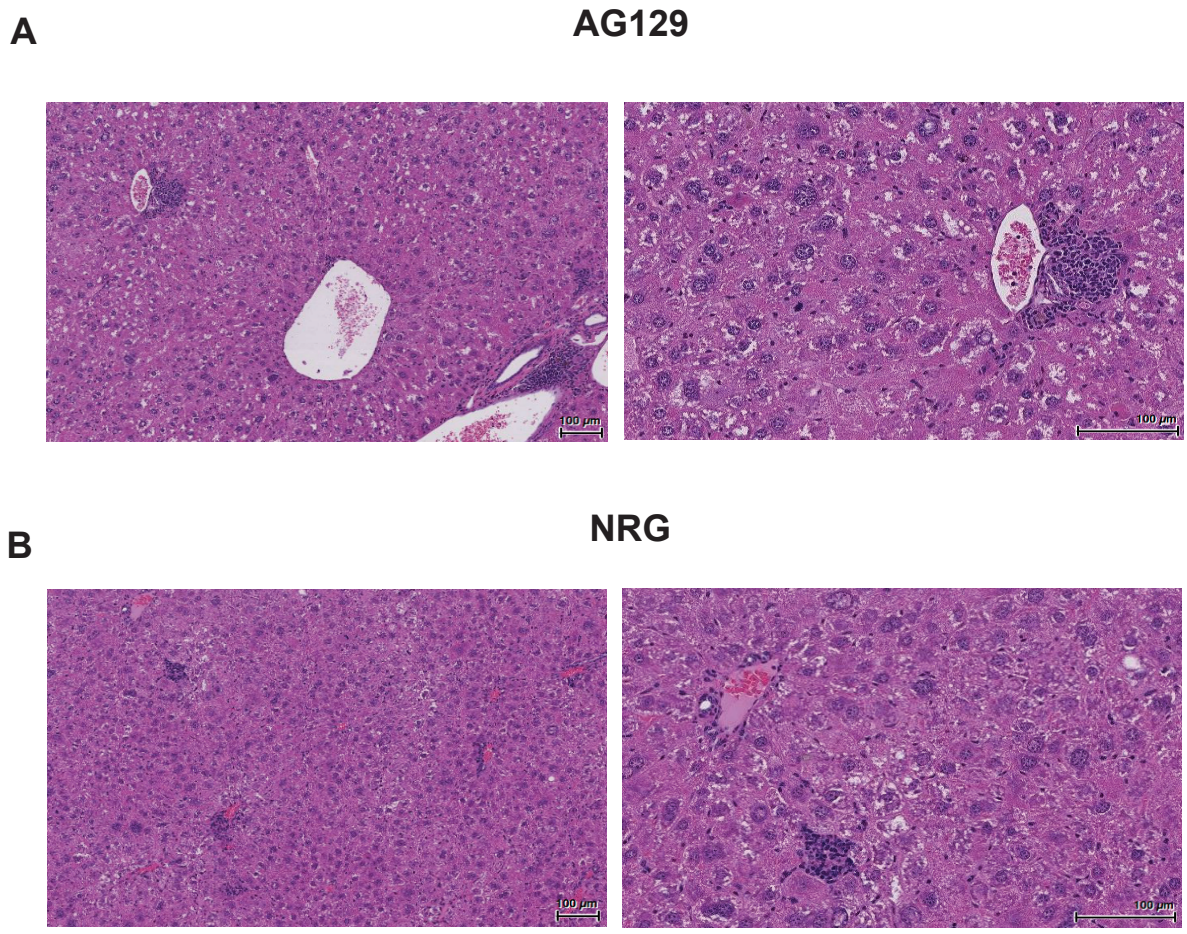

Fig. S3. Liver histology of chronically infected NRG and AG129 mice.

(A) Representative H&E staining of liver sections from AG129 mice infected with NrHV for 35 weeks. (B) Representative H&E staining of liver sections from NRG mice infected with NrHV for 35 weeks. Scale bars, 100µm.

Fig. S4

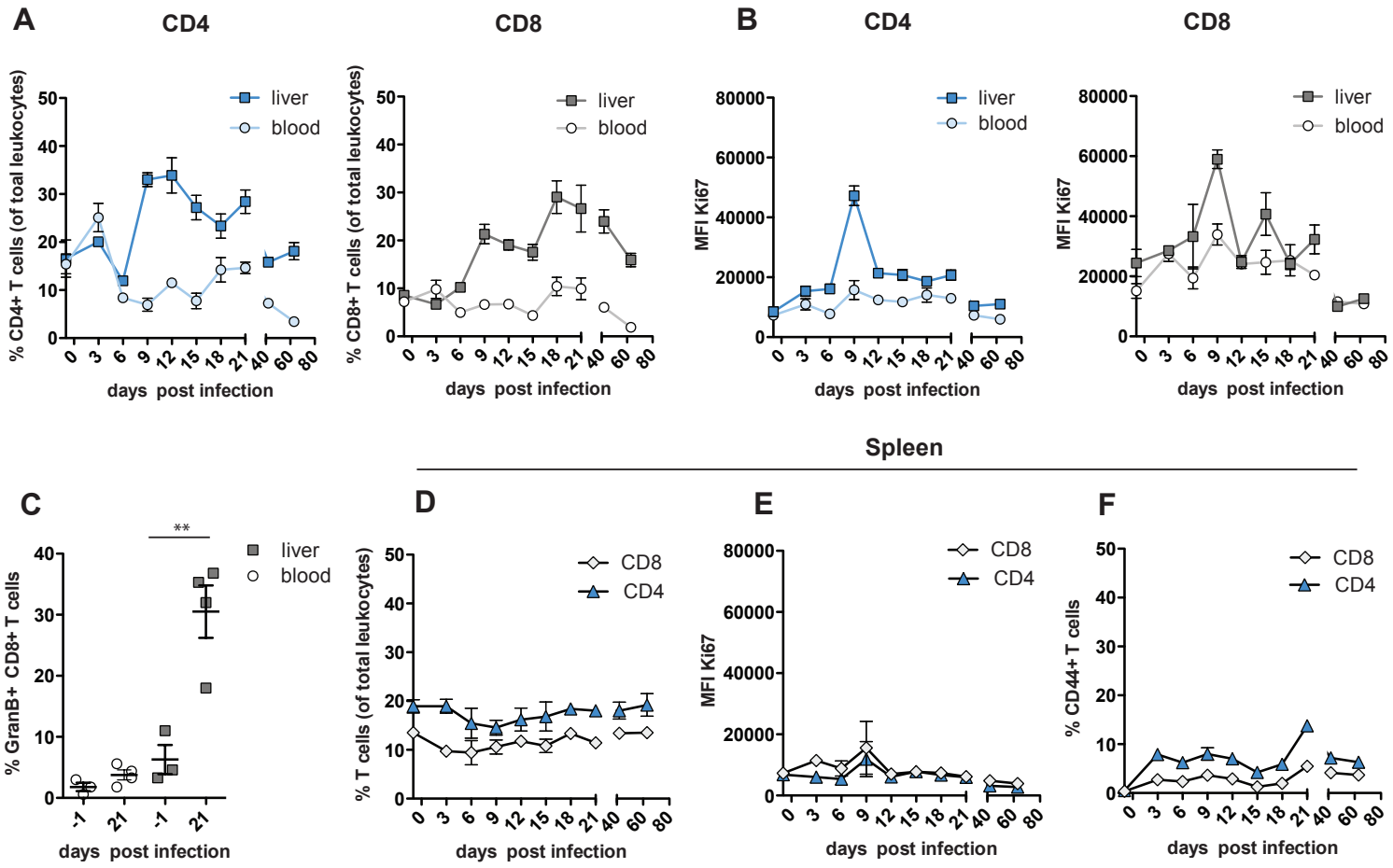

Fig. S4. T cell analysis during acute NrHV infection in immune-competent mice.

8-week-old C57BL/6J mice were infected i.v. with 10^4 GE of NrHV. (A) Frequencies of peripheral and hepatic CD4+ T cells (left) and CD8+ T cells (right) within the leukocyte population are shown and (B) Mean fluorescence intensity (MFI) of Ki67 staining in peripheral and hepatic CD4+ (left) and CD8+ (right) T cells during acute NrHV infection. (C) Frequencies of hepatic granzyme B-producing CD8+ T cells at 1 day prior and at day 21 p.i. (D-F) Frequencies of splenic CD4+ and CD8+ T cells within the leukocyte population (D) and Ki67 MFI (E), and CD44+ effector cell frequencies (F) within the splenic CD4+ and CD8+ T cell populations are shown. Representative data from 2 independent experiments with 4 mice per group (mean ±SEM) are shown. Statistics: unpaired students t-test: ** ≤ 0.001.

Fig. S5

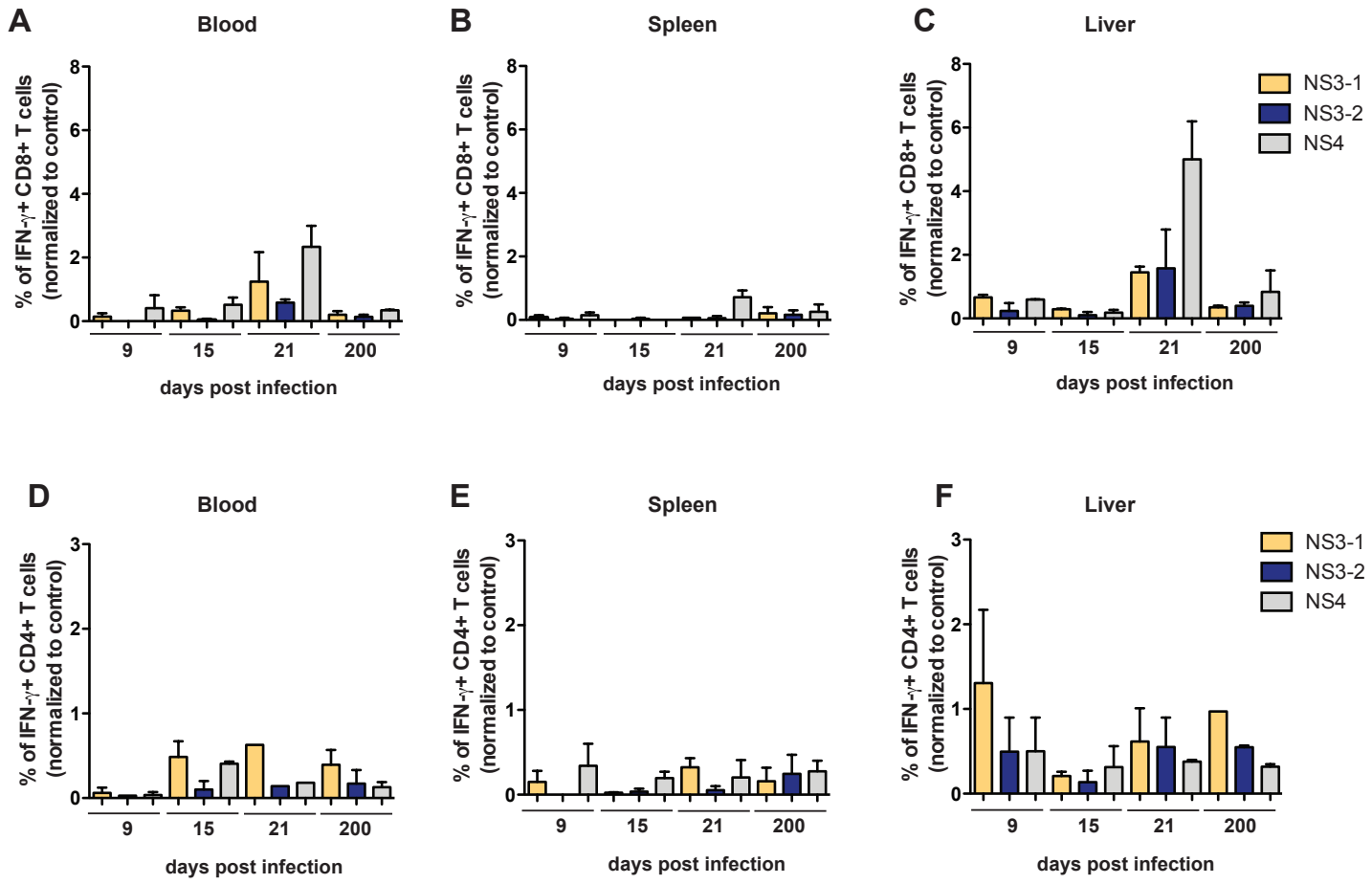

Fig. S5. Characterization of NrHV-specific CD4+ and CD8+ T cells during acute infection.

8-week-old C57BL/6J mice were infected i.v. with 10^4 GE NrHV. At multiple time points p.i. cells were isolated from blood, spleen and liver and stimulated ex vivo with 1μg/ml NrHV NS3-1, NS3-2 or NS-4 peptide pools or left unstimulated (control). After 5h of incubation cells were analyzed for intracellular cytokine production by FACS analysis. NrHV-specific IFN-γ production by peripheral, splenic and intrahepatic CD8+ (A-C) and CD4+ (D-F) T cells is shown. "Normalized to control" means that values of control were subtracted from each sample value. Representative data from 2 independent experiments with 3 mice per group (mean ±SEM) are shown.

Fig. S6

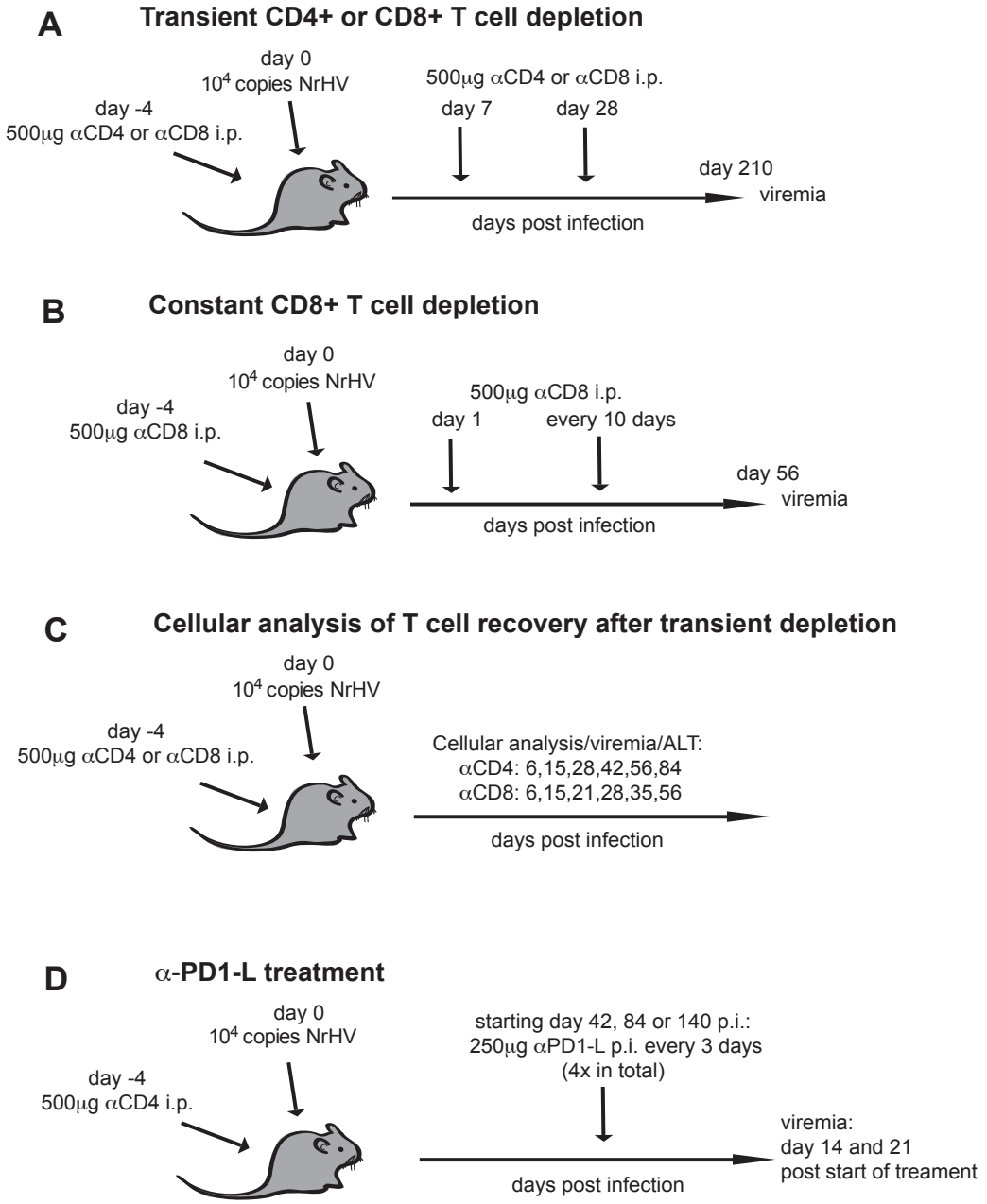

Fig. S6. Schematics of T cell depletion and PD-1L blockade experiments.

(A) Transient CD4+ or CD8+ T cell depletion using depleting antibodies. (B) Constant CD8+ T cell depletion using depleting antibodies. (C) Flow cytometric analysis of transient CD4+ or CD8+ T cell depletion and recovery during acute NrHV infection. (D) Blockade of PD-1:PD-1L interactions using a PD-1L blocking antibody during chronic NrHV infection.

Fig. S7

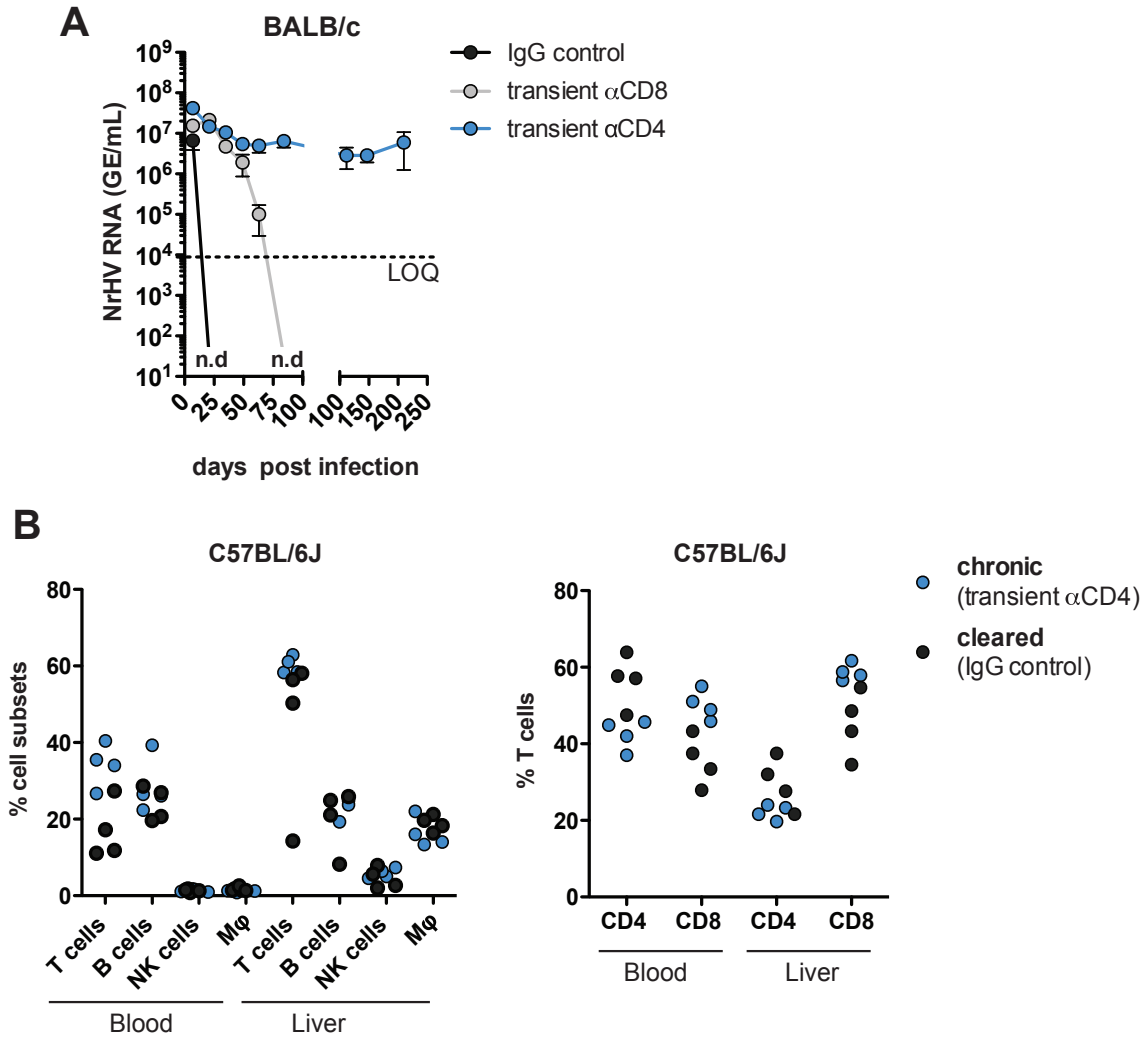

Fig. S7. T cell depletion and recovery during NrHV infection in immune-competent mice.

(A) 8-week-old BALB/c mice were transiently depleted (day 4 prior; day 7 and 28 p.i.) of CD4+ or CD8+ T cells using depleting antibodies and infected i.v. with 10^4 GE NrHV. Viremia was analyzed until day 210 p.i. Representative data from 3 independent experiments with 4 mice per group (mean ±SEM) are shown. (B) Flow cytometric analysis of peripheral and hepatic immune cell subsets (left) and T cell subsets (right) at day 210 p.i in C57BL/6J mice that were transiently depleted of CD4 T cells or received normal IgG as a control.

Fig. S8

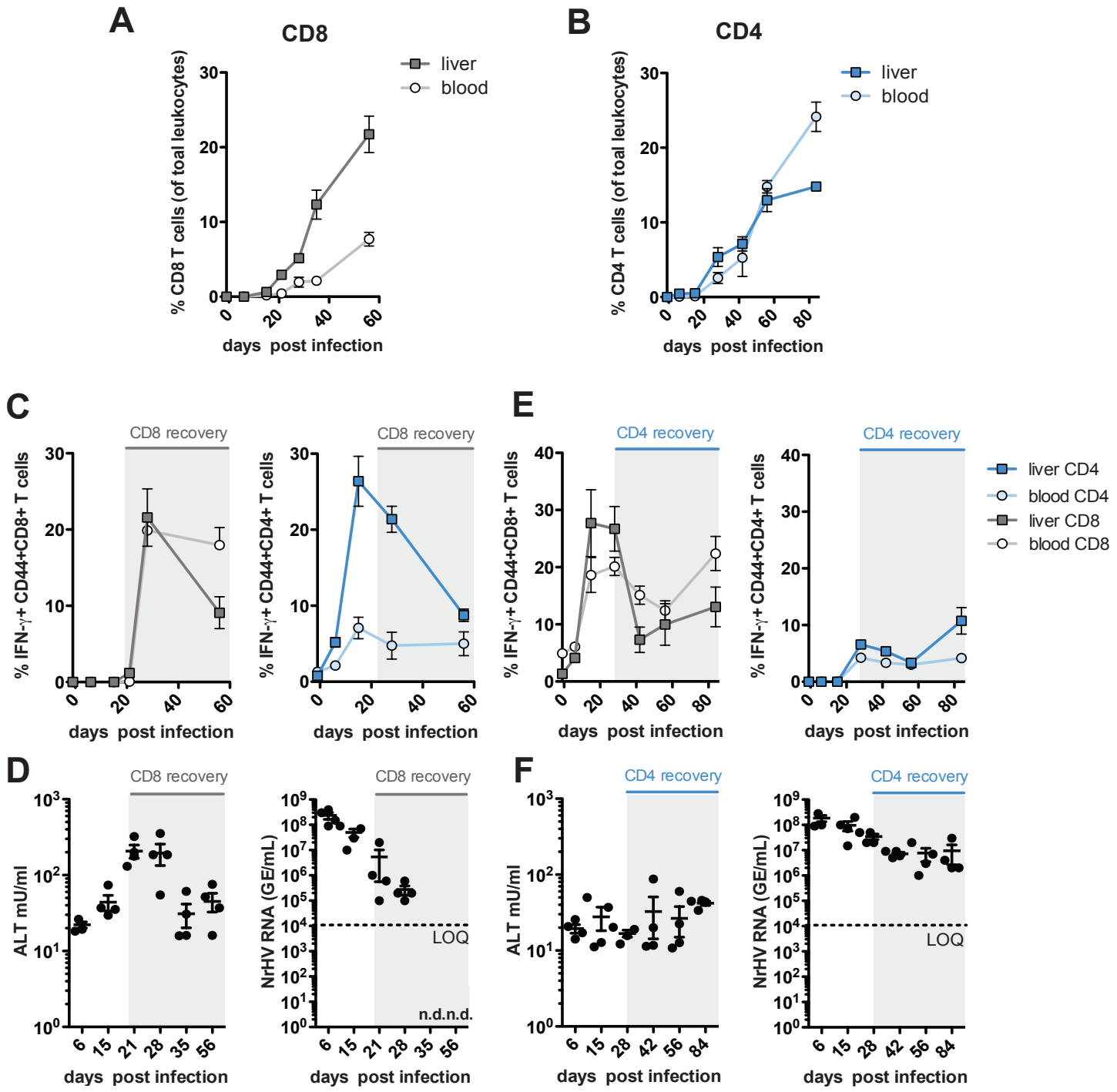
A
CD8
liver
blood
% CD8 T cells (of toal leukocytes)
days post infection
B
CD4
liver
blood
% CD4 T cells (of toal leukocytes)
days post infection
C
CD8 recovery
% IFN-γ+ CD44+CD8+ T cells
% IFN-γ+ CD44+CD4+ T cells
days post infection
E
CD4 recovery
% IFN-γ+ CD44+CD8+ T cells
% IFN-γ+ CD44+CD4+ T cells
days post infection
liver CD4
blood CD4
liver CD8
blood CD8
D
CD8 recovery
ALT mU/ml
NrHV RNA (GE/mL)
LOQ
n.d.n.d.
days post infection
F
CD4 recovery
ALT mU/ml
NrHV RNA (GE/mL)
LOQ
days post infection

Fig. S8. Analysis of NrHV infection during T cell recovery after initial depletion.
(A-B) Kinetics of peripheral and hepatic CD8+ (A) and CD4+ (B) T cell recovery after initial transient depletion at day 4 prior to infection. (C-F) Analysis of NrHV infection during recovery of CD8+ (C-D) or CD4+ (E-F) T cells after transient depletion (day 4 prior infection). (C) Frequencies of peripheral and hepatic IFNγ+CD44+ cells (PMA/Ionocyin stimulation) within the CD8+ (left) and CD4+ (right) T cell subset and (D) kinetics of ALT levels (left) and NrHV viremia (right) during CD8+ T cell depletion and recovery (shaded in grey). (E) Frequencies of peripheral and hepatic IFNγ+CD44+ cells within the CD8+ (left) and CD4+ (right) T cell subset and (F) kinetics of ALT levels (left) and NrHV viremia (right) during CD4+ T cell depletion and recovery (shaded in grey). Representative data from 2 independent experiments with 4 mice per group (mean ±SEM) are shown.

Fig. S9

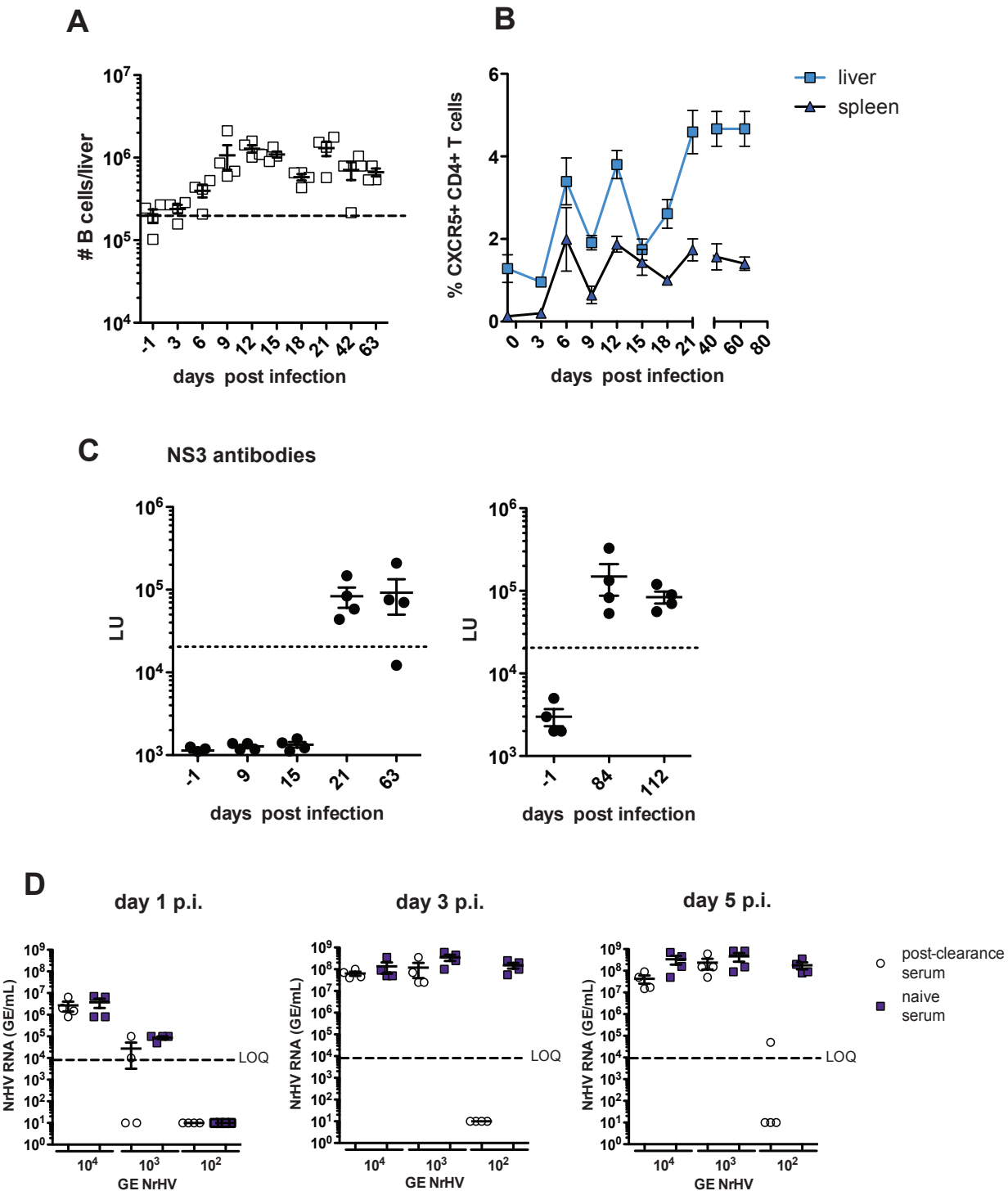
A
B cells/liver
days post infection
B
% CXCR5+ CD4+ T cells
liver
spleen
days post infection
C
NS3 antibodies
LU
days post infection
LU
days post infection
D
day 1 p.i.
day 3 p.i.
day 5 p.i.
NrHV RNA (GE/mL)
LOQ
GE NrHV
post-clearance serum
naive serum

Fig. S9. Analysis of neutralizing antibody production during acute NrHV infection.
(A-B) 8-week-old C57BL/6J mice were infected i.v. with 10^4 GE NrHV. Flow cytometric analysis of total numbers of intrahepatic B220+ B cells (A) and frequencies of CXCR5+ follicular T helper cells (B) during acute infection in liver and spleen. (C) LIPS (luciferase immunoprecipitation system) based detection of anti NrHV NS3 antibody titers in the serum of C57BL/6J mice. LU: light units. Dotted lines indicate negative cut-off. (D) 10^4, 10^3 and 10^2 GE NrHV were incubated for 1h at 37°C with either 5µl serum from naïve mice (naïve serum) or mice that previously cleared an NrHV infection with the same inoculum (post clearance serum). Subsequently naïve C57BL/6J mice were infected with 10^4, 10^3 or 10^2 GE pre-incubated virus. NrHV viremia at days 1, 3 and 5 p.i. is shown. Representative data from 2 independent experiments with 4 mice per group (mean ±SEM) are shown.

Fig. S10

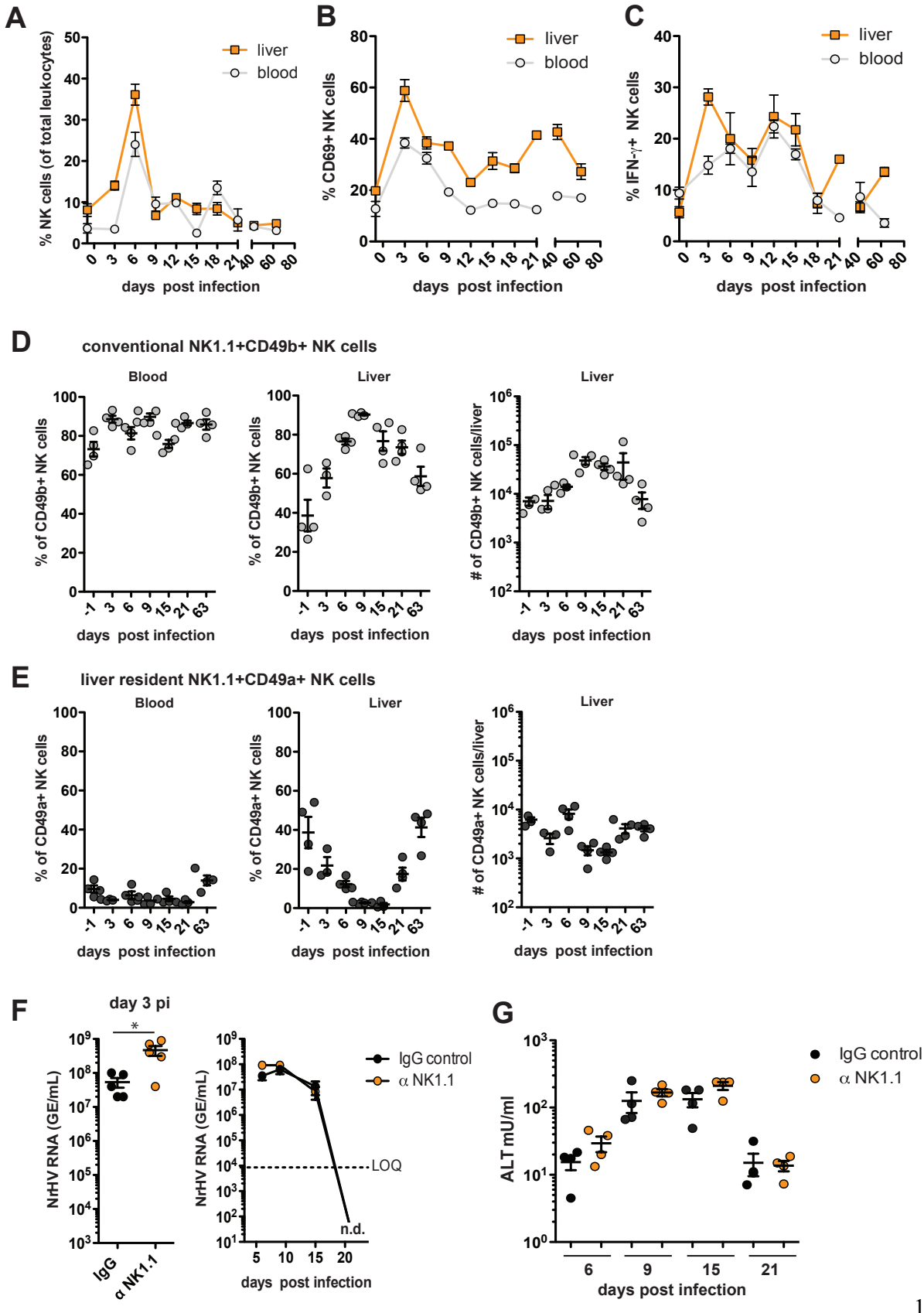
A
% NK cells (of total leukocytes)
liver
blood
days post infection
B
% CD69+ NK cells
liver
blood
days post infection
C
% IFN-γ+ NK cells
liver
blood
days post infection
D
conventional NK1.1+CD49b+ NK cells
Blood
% of CD49b+ NK cells
days post infection
Liver
% of CD49b+ NK cells
days post infection
Liver
# of CD49b+ NK cells/liver
days post infection
E
liver resident NK1.1+CD49a+ NK cells
Blood
% of CD49a+ NK cells
days post infection
Liver
% of CD49a+ NK cells
days post infection
Liver
# of CD49a+ NK cells/liver
days post infection
F
day 3 pi
*
NrHV RNA (GE/mL)
IgG
α NK1.1
NrHV RNA (GE/mL)
IgG control
α NK1.1
LOQ
n.d.
days post infection
G
ALT mU/ml
IgG control
α NK1.1
days post infection

Fig. S10. Conventional NK cells are expanded in the liver during acute NrHV infection, but are not essential for viral clearance.

8-week-old C57BL/6J mice were infected i.v. with 10^4 GE copies NrHV. (A-C) Flow cytometric analysis of blood- and liver-derived NKp46+ NK cells during acute NrHV infection. Overall frequencies of NKp46+ NK cells within the leukocyte population (A) and frequencies of CD69+ (B) or IFN-γ+ (C) cells within the NKp46+NK cell subset are shown. (D) Flow cytometric analysis of conventional NK1.1+CD49b+ NK cell frequencies in blood (left graph) and liver (middle graph) and total hepatic cell numbers (right graph) during acute infection. (E) Analysis of liver resident NK1.1+CD49a+ NK cell frequencies in blood (left graph) and liver (middle graph) and total hepatic cell numbers (right graph) during acute infection. (F-G) 8-week-old C57BL/6J mice were depleted of NK1.1 cells at day 2 prior to infection using a depletion antibody and infected with 10^4 GE copies NrHV. Viremia (F) and ALT levels (G) were analyzed at days 3, 6, 9, 15 and 21 p.i. and compared to control mice. Representative data from 2 independent experiments with 4 mice per group (mean ±SEM) are shown. Statistics: unpaired students t-test: * ≤ 0.01.

Fig. S11

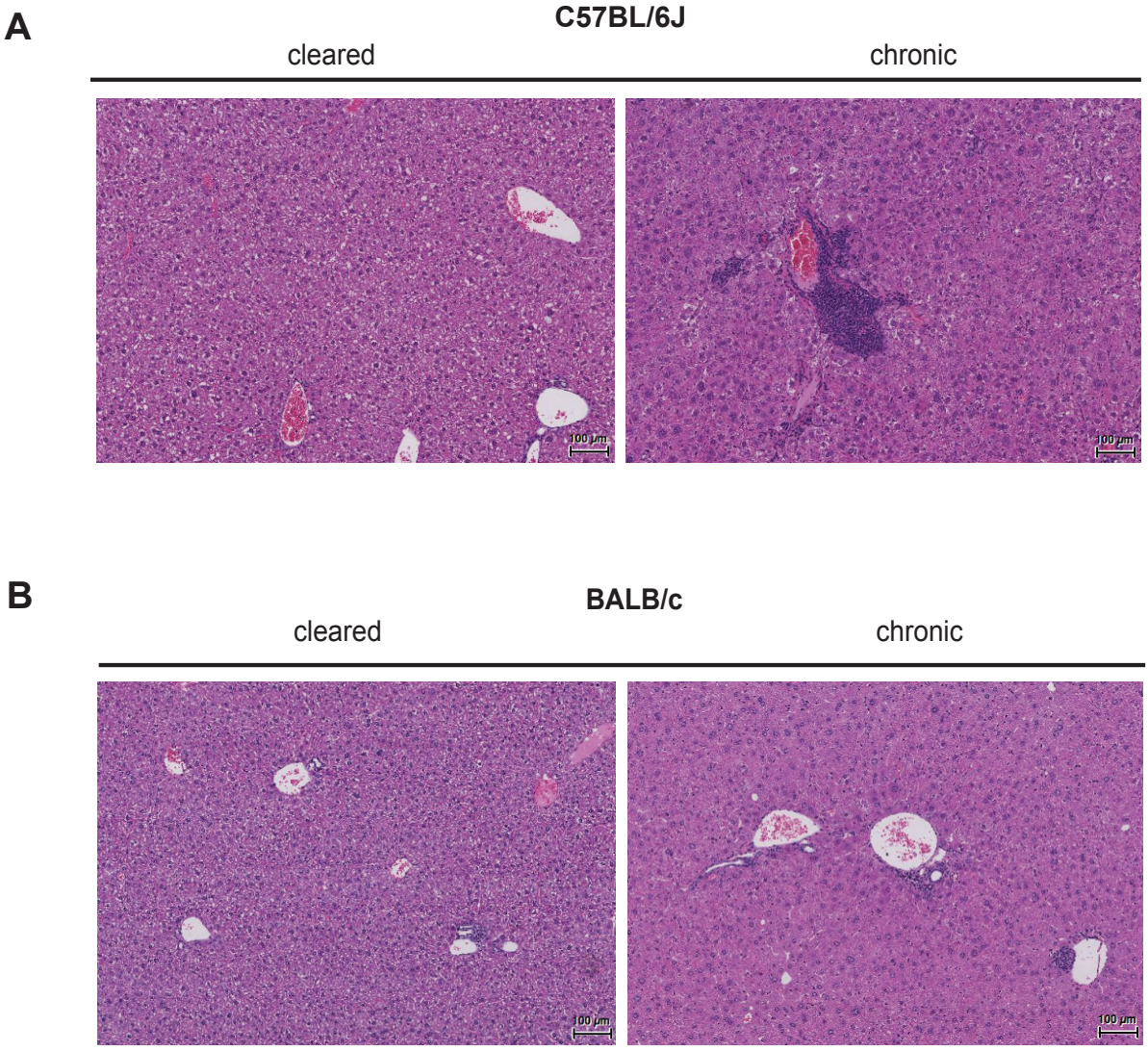

Fig. S11. Liver histology of chronically infected C57BL/6J and BALB/c mice.
(A) Representative H&E staining of liver sections at day 210 p.i. from C57BL/6J mice with acute resolving infection (left) or chronic infection after initial CD4+ T cell depletion (right). (B) Representative H&E staining of liver sections at day 210 p.i. from BALB/c mice with acute resolving infection (left) or chronic infection after initial CD4+ T cell depletion (right). Scale bars, 100µm.

Fig. S12

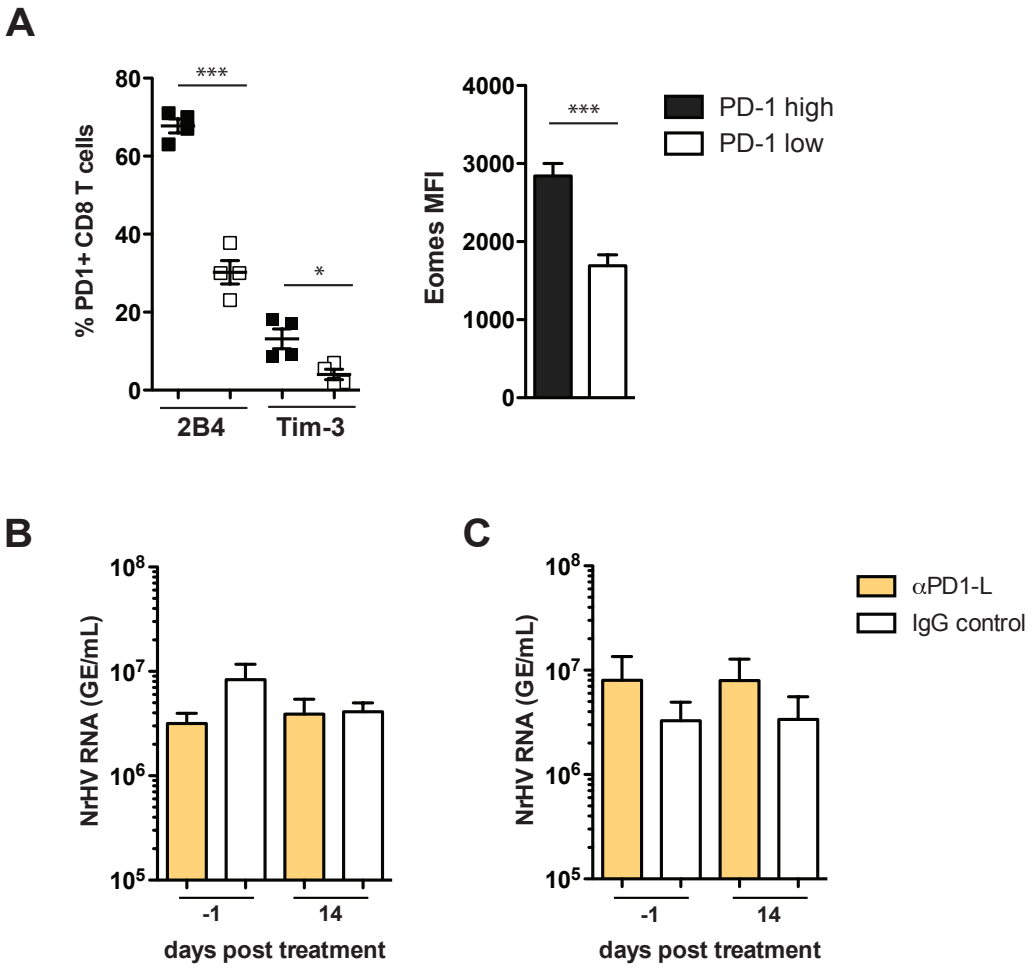

Fig. S12. Phenotypic analysis of PD-1+ T cells and PD-1L blockade during chronic NrHV infection.

(A) Flow cytometric analysis of hepatic CD8+ T cells from C57BL/6J mice chronically infected for 210 days. The left graph shows 2B4 and Tim-3 expression on PD-1^{high} and PD-1^{low} cells. The right graph shows MFI (mean fluorescence intensity) of Eomes staining in PD-1^{high} and PD-1^{low} cells. (B-C) Chronically infected C57BL/6J mice were treated with a PD-1L blocking antibody or appropriate IgG control starting at day 84 (B) or day 140 (C) p.i. NrHV viremia was analyzed at day 1 prior to the start of treatment and compared to viremia at day 14. Representative or combined data from 2-5 independent experiments with 4-5 mice per group (mean ±SEM) are shown. Statistics: unpaired students t-test: * ≤ 0.01, *** ≤ 0.0001.

Additional Data table S1 (separate file)

Summary of all consensus-coding mutations found in individual mice

Left columns show nucleotide position in the ORF, the reference nucleotide and alternative nucleotide. M7-M15 are 5th passage NRG mice from which the serial pool was made and M31-M34 are challenged C57BL/6J mice at week one p.i. (marked in blue). For each mouse, the amino acid changes by at least 50% (numbered according to the polyprotein) are shown if present and putative adaptive changes in bold. No change is indicated as (-). Additionally, the detected variant frequency (%) of the rat inoculum is in the far right column; (-) indicates not detected (<0.1%).

Additional Data table S2 (separate file)

Comparison of coding changes in serum pools by deep sequencing

For the cumulative coding changes at each codon, the amino acid residue numbering (Pos.AA, according to the polyprotein), first nucleotide in codon (Pos.nt.first, according to the ORF), last nucleotide in codon (Pos.nt.last), rat inoculum reference codon (Codon_Ref) and rat reference amino acid (AA_Ref) are shown. The cumulative frequency of coding changes at each codon is shown for the Rat inoculum and both NRG serum pools. The $\log_2$-transformed relative frequency between each pool and the rat inoculum are shown for all amino acid variants. For this calculation, a pseudo-count of 0.5% was added to the deep sequencing data before calculation to reduce noise from low abundant variants.